

Chapter 10

Soil Profile Imaging for Estimating the Depth Distributions of Clay, Iron, and Hydrological Conditions of Soils Under Rice in Northern Taiwan

Shih-Hao Jien, Zeng-Yei Hseu, Chen-Chi Tsai and Zueng-Sang Chen

Abstract Soil color variation, clay illuviation, and translocation of Fe and Mn are influenced by hydrological conditions. Soil profile imaging has been considered to predict the distribution of clay, Fe and Mn oxides, and hydrological conditions. Ten Ultisol and Alfisol profiles were selected at elevations ranging from 15 m to 40 m a.s.l. at Chungli Terrace, northern Taiwan. Sixty soil horizons were collected for redoximorphic features (RMFs) identification and analysis of soil texture and selective extraction of Fe and Mn oxides. All soil properties were correlated with the RMFs. There was a significantly positive correlation between gray mottle (GM) (value ≥ 5 , chroma ≤ 3) amounts and annual reduction duration (ARD) ($r = 0.80^{**}$, $p < 0.01$) and a negative correlation between red mottle (RM) (value ≥ 4 , chroma ≥ 3) amounts and ARD ($r = 0.75^{**}$, $p < 0.01$) at surface horizons (within 30 cm). A significantly positive correlation was also found between RM and clay content ($r = 0.32^*$, $p < 0.05$), indicating clay might determine the formation of RM. Moreover, the ratios of iron activity (Fe_o/Fe_d) and iron crystalline ($(Fe_d - Fe_o)/Fe_t$) could also be good indices for ARD prediction. The Mn_d/Fe_d seemed an index of frequent fluctuation of water table in soil profiles. Using image analysis technique, replacing naked eye identification of RMF could improve correlations between soil color and hydrological conditions.

Keywords Pedogenesis Hydrological condition · Redoximorphic feature · Soil color · Digital soil morphometrics

S.-H. Jien

Department of Soil and Water Conservation, National Pingtung University of Science and Technology, Pingtung 91201, Taiwan

Z.-Y. Hseu · Z.-S. Chen (✉)

Department of Agricultural Chemistry, National Taiwan University, Taipei 10617, Taiwan
e-mail: soilchen@ntu.edu.tw

C.-C. Tsai

Department of Forestry and Natural Resources, National Ilan University, I-Lan 26047, Taiwan

10.1 Introduction

Digital soil morphometrics is defined as the application of tools and techniques for measuring and quantifying soil profile attributes (horizons, texture, color, structure, moisture, mottles, consistence, carbonates, rock fragments, pores, and roots) and deriving continuous depth functions (Hartemink and Minasny 2014). Technologies that can rapidly characterize the entire soil profile are necessary (Ben-Dor et al. 2008; Demattê et al. 2004; Stockmann et al. 2014; Viscarra Rossel and Webster (2011). Several digital techniques, including ground penetrating radar (GPR), electrical resistivity (ER), cone penetrometer, hyperspectral core scanner, and X-ray fluorescence (XRF), have been developed to supplement traditional ones to characterize soil profiles (Hartemink and Minasny 2014).

Soil color is considered a common property to depict soil horizons and classify soils. Soil color (matrix color/redoximorphic features, RMFs) could be used as an indicator of soil organic carbon content, drainage, aeration, iron content, or mineralogy, particularly in soils with lowland rice and frequent fluctuation of groundwater. The rice-growing soil is a hydric soil, which is defined as soils formed under conditions of sufficient saturation or flooding during the growing season to develop an anaerobic condition in the upper part of the soil. The rice-growing hydric soils are characterized by hydrological conditions and various soil colors in their matrix (Hseu and Chen 2001; Jien et al. 2010). The development of suitable color indices or a good digital technique for color descriptions in situ could effectively identify soil moisture regimes (SMR) and be helpful for the classification of hydric soils.

Generally, gray mottles (GMs) or depleted matrix (chroma 2) has been considered as generally indicators for extensive duration of saturation and reduction (Daniel et al. 1971; Simonson and Boersma 1972; Cox et al. 1996; Jien et al. 2010). Franzmeier et al. (1983) found that GMs with chroma 2 indicated saturation for 30 % of the year for loamy soils in Indiana, USA. Cycles of reduction and oxidation in soils over prolonged periods and the consequent mobility and accumulation or depletion of Fe and Mn resulted in the formation of RMFs (Fanning and Fanning 1989; Vepraskas 1992; Hseu and Chen 1996; Jien et al. 2004, 2010). Studies have tested the application of RMFs as SMR indicators in various environments. High levels (7.5 %) of Fe and Mn concretions were found in the upper B horizons of soils along hydrosequences in Bavaria, Germany (Schwertmann and Fanning 1976). In a study of five fine-silty soils in Indiana, iron depletions with chroma 2 indicated >30 % saturation at a depth of one meter (Franzmeier et al. 1983). In hardwood forest areas in Louisiana, USA, soils with chroma <2 with redox concentrations below the A horizon generally indicated hydric conditions constituting saturation and reduction >25 % of the growing season (Faulkner and Patrick 1992).

The relationship between soil color and SMR might be failed because of wrong judgment of soil colors by naked eyes. The digital techniques for soil morphometrics might improve judgments. Recently, soil color has been measured indirectly using Vis-NIR. Viscarra Rossel et al. (2009) used Vis-NIR to measure soil color

in situ and in the laboratory. Measurements were compared to the Munsell color chart readings. There was fair agreement between spectroscopic estimates of soil color and Munsell readings although Vis–NIR tended to be slightly darker and more yellow. Ben-Dor et al. (2008) used Vis–NIR field spectrometer and an accessory to read subsoil reflectance to examine soil color in Alfisols, Inceptisols, and Vertisols. The results were compared to traditional soil descriptions, and it was possible to describe quantitatively and objectively the soil profile color in situ using optical instruments.

Quantitative descriptions of RMFs associated with hydromorphology for the rice-growing soils in Taiwan have been studied by Hseu and Chen (1996, 2001) and Jien et al. (2004, 2010). Soils had high chroma matrix colors, Fe (chroma 6) and Mn (chroma 1) concentrations, and chroma 1 depletions > horizons that were saturated for considerable periods were reduced for a much shorter time. Some problems exist regarding long-term assessment and interpretation of the criteria, particularly in seasonally saturated rice-growing soils. This study attempts (1) to compare the RMFs of rice-growing soils with different elevations, (2) to clarify the correlations between soil colors and local hydrology condition of lowland rice-growing soils in Taiwan, (3) to compare the digital data, including types and quantities of RMFs, identified by naked eyes and image analysis.

10.2 Materials and Methods

10.2.1 Site Description

The study area is located inside the Chungli Terrace in northern Taiwan, about 40 km southwest of Taipei city (Fig. 10.1). The altitude ranges from 20 to 40 m above sea level. The soil is developed on an alluvial terrace from Quaternary, with a minimum thickness of 5 m (Ho 1988). The mean air temperature is 27 °C in summer and 13 °C in winter. Average annual rainfall is 1560 mm, and the annual rainfall exceeds the annual evapotranspiration.

Ten representative rice-growing soils were selected for this study. Plinthite was found only in Pingchen soil, and other soils contained plinthitic feature (Fig. 10.2). All pedons were close (~2 km) to the seashore. Slopes range from 2 to 6 % over 2 km. All soils are classified as Ultisols or Alfisols according to the Keys to Soil Taxonomy (Soil Survey Staff 2010), and specifically, they are Oxyaquic Paleudult (Pingchen), Plinthitic Paleudalf (Tachuwei), Plinthaquic Paleudult (Lungchung), Typic Plinthaqualf (Chuwei-1), Typic Plinthaquult (Luchu, Hsinwu, and Houhu-1), and Typic Paleaquult (Houko, Chuwei-2 and Houhu-2). The Pingchen, Lungchung, and Tachuwei series are the farthest from the seashore (about 4 km) and are situated at the highest elevation (around 40 m) in this study area. The Houhu-1, Houko, Chuwei-2, and Houhu-2 series are the nearest to the seashore and have the lowest elevation (15–20 m). The Chungli Terrace has been used for rice (*Oryza sativa* L.)

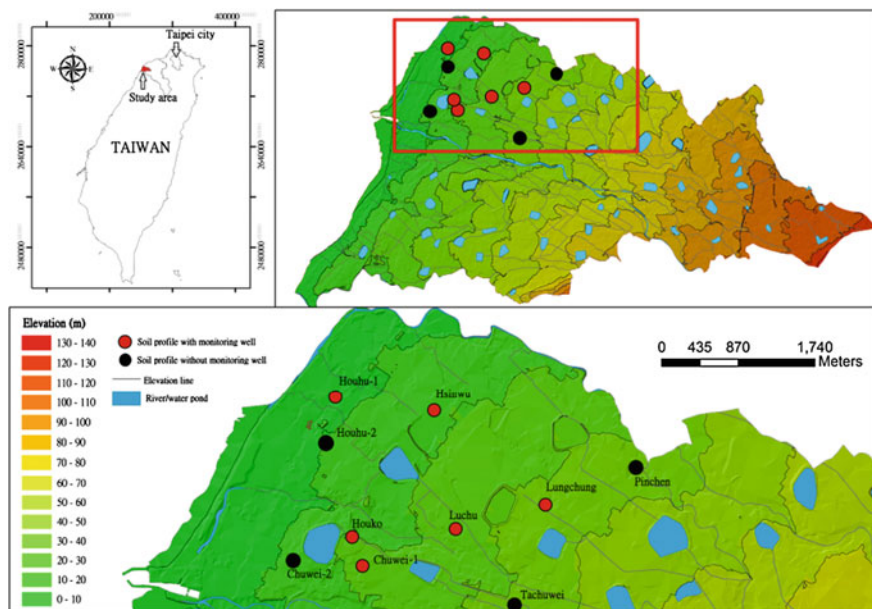


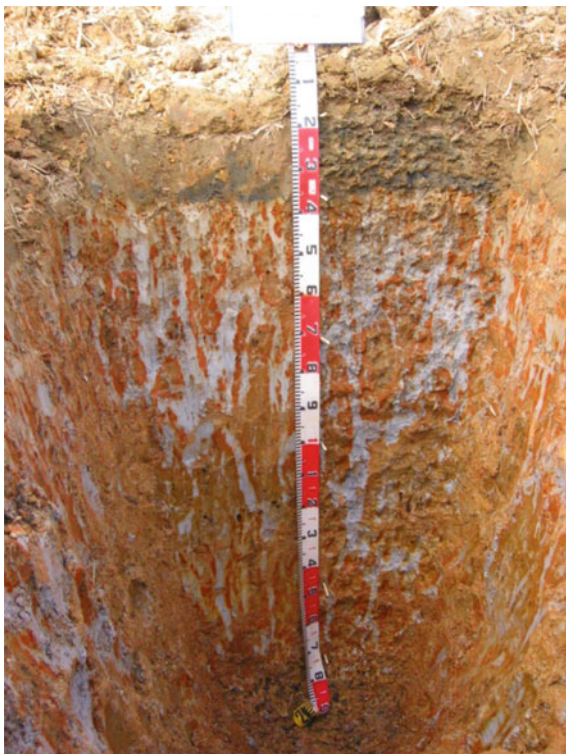
Fig. 10.1 Locations of the studied pedons at Chungli Terrace in northern Taiwan

cultivation since the 1950s. Each year, rice is harvested during the March to October growing season, and the soils are fallowed in winter. The soils are seasonally flooded by irrigation water and groundwater.

10.2.2 Soil Analyses

Soil pits were excavated in 1996 and in 2002 and 2003. The description included morphological characteristics and RMFs based on the Soil Survey Manual (Soil Survey Staff 1993). The soil properties are given in Hseu and Chen (2001) and Jien et al. (2004, 2010). Fe oxides (Fe_d) and Mn oxides (Mn_d) were extracted by the dithionite–citrate–bicarbonate (DCB) method (Mehra and Jackson 1960). Amorphous Fe (Fe_o) and Mn (Mn_o) were extracted by 0.2 M ammonium oxalate (pH = 3.0) (AAO) (McKeague and Day 1966). All elements were determined using an atomic adsorption spectrometer (Hitachi, 180-30 type). Total contents of Fe (Fe_t) and Mn (Mn_t) were measured after digestion with $HF-HClO_4-H_2SO_4-HCl$ on a hot plate (200 °C) (Hossner 1996). The bulk density of each size fraction of the ferromanganiferous nodules was also determined by the paraffin clod method (Blake and Hartge 1986). Bulk density was determined on six samples for 2- to 5-mm nodules and three samples for other, larger size fractions. All soil analyses were performed in triplicate.

Fig. 10.2 The plinthitic feature of rice-growing soils in our study area. The photograph is Chuwei-1 pedon



10.2.3 Hydrological Monitoring

In six of the ten soils, a 7×7 m plot was established to monitor hydrological conditions over two years, which Lungchung–Hsinwu–Houhu-1 monitored during 1996–1997, and Luchu–Chuwei-1–Houko monitored during 2004–2005. The following data were recorded at biweekly intervals: (1) water table level, (2) soil water tension at depths of 25, 75, 100 and 200 cm, and (3) soil redox potential at depths of 25, 75, 100, and 200 cm. All data were recorded in triplicates. Hydrological data at other pedons were used for the nearest pedons in which no measurements were made.

Plowing in lowland rice forms compact subsurface layers, and perched water appears during the growing seasons. These compact layers exhibit lower saturated hydraulic conductivity than the overlying horizon and water tends to accumulate above them, creating a perched zone of saturation. Wells were constructed to measure the perched water table, and piezometers were used to determine water table depths. Tensiometers and platinum electrodes were installed at predetermined depths and used to monitor saturation and redox potential (Eh). The voltage reading was recorded after the drift decreased to equilibrium, characterized by less than

5 mV of change during a 10-s period. The field reading was adjusted by adding +200 mV in order to correct for reference electrode potential. The threshold Eh value for the reduction of Fe (III) to Fe (II) was estimated from an Eh–pH diagram and equation, $1235 - 177 \text{ pH}$ (for $\text{pH} < 7.5$), which was provided by Ponnampertuma (1972). Also, the range of pH (5.0–6.0) in the studied soils was measured to establish pH-corrected redox threshold levels for Fe (II). Instruments were constructed in triplicate for each study site (including wells, piezometers, and tensiometers). All measurements were made at biweekly intervals and in triplicate at each monitoring time.

10.2.4 Identification of Redoximorphic Features by Image Analysis

Five aluminum boxes measuring $10 \times 10 \times 8$ cm were used for collecting the soil blocks from each soil horizon of the pedons of Luchu, Chuwei-1, and Houko. Fresh soil blocks from two boxes were taken out for image analysis, and other three boxes were oven-dried at 105°C for 24 h to remove water before sieving the ferromanganiferous nodules. A stainless wire was used to cut the soil blocks with an interval of 1 cm. Eight soil pieces were extracted from each soil block, and pictures were taken for image analysis. ERDAS Imagine 8.4 (ERDAS, USA) was used for image analysis.

10.3 Results and Discussion

10.3.1 Soil Morphology and Hydrological Conditions

The soils were divided into three groups based on their soil morphological characteristics (Table 10.1). The first group (around 40 m a.s.l.) included Pingchen, Tachuwei, and Lungchung soils, which had no plinthite or plinthite ranged from 2 to 50 % within 150 cm depth. The soils of Luchu, Hsinwu, Chuwei-1, and Houhu-1 are located at the elevation around 20–40 m.a.s.l. and characterized by plinthite, and most soil horizons (20–200 cm in depth) contained plinthite. The third group (15–20 m a.s.l.) included Houko, Chuwei-2, and Houhu-2 soils, and the morphological features were different as gleyzation was the dominant soil forming process due to long-term high groundwater table. The Btg as the major soil horizon and the reduced matrix (chroma ≤ 2) of the Ap and Btg horizons indicated strongly reduced conditions.

All pedons had a perched water table during the growing season from March to November. Table 10.2 shows the annual duration of saturation and reducing conditions at different depths. In the first soil group, the least annual reduction duration ($\sim 5\%$) was found in the lower soil horizons, which corresponded with the color

Table 10.1 Morphological characteristic of ten pedons in study area

Horizons	Depth (cm)	Moist color	Soft masses [†]	Depletions	Texture	Boundary [‡]
<i>Pinchen (Oxyaquic Paleudult)</i>						
Ap	0-20	10YR 4/4	FP 5YR 5/8 (15 %) [§]	- [¶]	-	-
AB	20-40	10YR 4/4	FP 5YR 5/8 (15 %)	-	-	-
Bt1	40-60	7.5YR 5/8	-	MP 5Y 5/3 (15 %)	-	-
Bt2	60-100	10R 3/6	MP 10YR 5/6 (40 %)	M&FP 5Y 5/3 (<2 %)	-	-
Bt3	100-130	10R 3/6	M&CP 10YR 7/4 (30 %)	-	-	-
Bt4	130-160	2.5YR 4/8	M&CP 10YR 7/4 (30 %)	-	-	-
Bt5	160-200	2.5YR 4/8	M&CP 10YR 7/4 (30 %)	MP 2.5Y 8/2 (20 %)	-	-
<i>Tachuwai (Plinthitic Paleudalf)</i>						
Ap	0-35	10YR 5/6	FP 10R 4/6 (2 %)	-	L	-
AB	35-60	2.5Y 6/6	MP 10R 4/8 (40 %)	-	C	-
Bt1	60-80	2.5YR 4/8	MP 7.5YR 6/8 (25 %)	-	SiL	-
Bt2	80-120	10YR 7/8	MP 2.5YR 4/8 (30 %)	-	SiL	-
Bt3	120-150	2.5YR 3/6	MP 7.5YR 5/8 (20 %)	MP 5YR 7/2 (30 %)	SiL	-
<i>Lunchung (Plinthaquic Paleudult)</i>						
Ap	0-20	2.5Y 4/2	-	-	SiCL	as
Bw	20-41	10YR 5/2	CD 5YR 5/8 (5 %)	-	SiC	aw
2A	41-56	10YR 4/2	CP 2.5YR 3/4 (5 %)	-	SiCL	cw
2Bt	56-85	10YR 4/4	CD 7.5YR 5/6 (10 %)	-	SiC	d
2Btv1	85-100	10YR 5/3	CP 2.5YR 5/8 (30 %)	CD 2.5YR 2.5/2 (5 %)	SiC	as
2Btv2	100-140	10YR 6/2	MP 2.5 YR 5/6 (20 %)	CP 2.5YR 2.5/2 (5 %)	SiC	d
2Btv3	140-180	10YR 6/1	MP 2.5 YR 5/8 (20 %)	CP 2.5YR 6/1 (20 %)	SiC	d
2Btv4	>180	10YR 6/1	MP 2.5 YR 5/8 (30 %)	CP 2.5YR 6/1 (15 %)	SiC	-
<i>Luchu (Typic Plinthaquult)</i>						
Ap	0-20	5Y 4/2	-	M&Cf 5YR 6/2 (20 %)	CL	cs
Btv1	20-50	2.5Y 6/1	M&Cd 2.5Y 5/6 (30 %); M&Cp 10YR 5/4 (10 %)	-	CL	d
Btv2	50-75	5Y 7/1	C&VCp 10YR 6/8 (30 %); M&Cp 5YR 5/8 (15 %)	-	CL	d
Btv3	75-104	5Y 8/1	M&Cp 5YR 5/8 (15 %); M&Cd 2.5Y 6/6 (20 %)	-	CL	d

(continued)

Table 10.1 (continued)

Horizons	Depth (cm)	Moist color	Soft masses [†]	Depletions	Texture	Boundary [‡]
Btv4	104-124	2.5Y 7/1	M&Cd 2.5Y 6/6 (25 %)	-	C	d
Btv5	124-160	5Y 7/1	F&Mp 2.5YR 4/8 (10 %); Md 2.5Y 6/6 (30 %)	-	C	d
<i>Hsinwu (Typic Plinthaquult)</i>						
Ap	0-15	2.5Y 4/3	-	-	SiL	cs
AB	15-26	2.5Y 4/1	-	CF 2.5Y 4/2 (10 %)	SiL	cs
Bt1	26-45	10YR 5/4	CD 7.5YR 4/4 (10 %); FF 10YR 5/8 (5 %)	-	SiC	d
Bt2	45-75	10YR 5/6	CD 5YR 5/8 (15 %); FF 10YR 5/8 (5 %)	-	SiC	aw
Btv1	75-107	10YR 5/2	MP 2.5YR 4/4 (25 %); MF 10YR 5/3 (5 %)	-	CL	d
Btv2	107-133	2.5YR 4/8	CD 10YR 6/3 (5 %)	CP 10YR 6/2 (5 %)	C	d
Btv3	133-160	2.5YR 4/8	CD 2.5YR 2/1 (5 %)	CP 10YR 6/2 (10 %)	C	d
<i>Chuwei-1 (Typic Plinthaquultf)</i>						
Ap	0-18	10YR 4/3	VF&Fp 10YR 6/8 (15 %)	-	C	cs
AB	18-36	2.5Y 3/2	VFp 7.5Y 6/8 (15 %)	-	CL	d
Btv1	36-70	2.5Y 7/1	M&Cp 5YR 4/8 (20 %); M&Fp 10YR 5/4 (10 %)	-	C	d
Btv2	70-110	2.5Y 7/1	M&Cd 2.5YR 4/8 (35 %); M&Fp 10YR 5/6 (25 %)	-	C	d
Btv3	110-145	2.5Y 7/1	C&VCp 10YR 5/8 (50 %); Cp 10YR 6/8 (30 %)	-	C	d
Btv4	145-170	2.5Y 7/1	V&VCp 2.5Y 5/8 (20 %); Mp 7.5YR 6/8 (45 %)	-	C	d
Btv5	170-200	2.5Y 7/2	-	-	C	d
<i>Houhu-1 (Typic Plinthaquult)</i>						
Ap	0-34	2.5Y 4/2	MP 5YR 4/4 (30 %)	-	CL	as
AB	34-47	2.5Y 4/1	CP 7.5YR 5/8 (10 %)	-	SiCL	cs
Bt1	47-66	10YR 4/3	MP 7.5YR 5/8 (10 %)	-	SiCL	cs
Btv1	66-82	10YR 5/3	MP 7.5YR 5/8 (10 %)	CD 10YR 6/1 (10 %)	SiC	g
Btv2	82-102	10YR 6/1	MP 2.5YR 5/8 (25 %)	-	SiC	d
Btv3	102-122	7.5YR 6/1	MD 2.5YR 5/8 (25 %)	MD10YR 7/1 (10 %)	SiC	d
Btv4	>122	7.5YR 6/1	MD 5YR 5/8 (30 %); MF 7.5YR 5/6 (20 %)	-	C	d

(continued)

Table 10.1 (continued)

Horizons	Depth (cm)	Moist color	Soft masses [†]	Depletions	Texture	Boundary [‡]
<i>Houko (Typic Paleaquilt)</i>						
Ap	0-20	10YR 4/4	p 2.5YR 5/8 (10 %)	-	C	gs
Bt1	20-50	2.5Y 4/2	F&Mp 5YR 5/6 (10 %)	F&Md 2.5Y 6/1 (15 %)	SiC	gw
Bt2	50-75	10YR 4/1	F&Mp 5YR 6/8 (10 %)	M&Cd 2.5Y 6/1 (15 %)	SiC	gw
Bt3	75-110	5Y 5/1	M&Cp 2.5YR 4/6 (30 %)	-	SiC	d
Btg1	10-130	10BG 4/1	F&Mp 10YR 6/6 (10 %)	-	SiC	d
Btg2	130-170	10BG 4/1	F&Mp 10YR 6/6 (2 %)	-	C	d
Btg3	170-200	10BG 4/1	F&Mp 10YR 6/6 (2 %)	-	C	d
<i>Chuwai-2 (Typic Paleaquilt)</i>						
Ap	0-35	7.5YR 4/6	CP 7.5YR 5/8 (10 %); FP 2.5YR 5/8 (<2 %)	-	SiL	-
AB	35-65	10YR 5/4	CP 7.5YR 6/8 (15 %)	-	SiL	-
Btg1	65-90	5G 5/1	MP 10YR 7/8 (30 %)	-	SiCL	-
Btg2	90-105	5PB 6/1	CP 10YR 7/8 (10 %)	-	SiCL	-
Btg3	105-120	5PB 6/1	CP 2.5Y 7/6 (4 %)	-	SiC	-
<i>Houhu-2 (Typic Paleaquilt)</i>						
Ap	0-25	10YR 6/2	FP 5YR 5/8 (10 %)	-	SiCL	-
Bt1	25-45	2.5Y 4/4	MP 5YR 5/8 (10 %)	-	SiC	-
Btg2	45-70	2.5Y 6/2	MP 5YR 5/8 (40 %)	-	SiC	-
Btg3	70-110	10YR 6/1	MP 2.5YR 5/8 (40 %)	-	SiC	-
Btg4	110-140	5 PB 6/1	MP 10YR 5/8 (20 %); MP 2.5YR 5/8 (20 %)	-	SiC	-

[†]F = fine, M = medium, C = coarse, p = prominent, d = distinct, f = faint

[‡]a = abrupt, c = clear, d = diffuse, g = gradual, s = smooth, w = wavy

[§]The value in parentheses is quantity of redoximorphic features

[¶]None

Table 10.2 Annual saturation and reduction duration of the studied soils

Soils	Elevations (m)	Soil depth (cm)	Annul saturation duration (%)	Annul reduction duration (%)
Pinchen (Oxyaquic Paleudult)	50	25	75	70
		50	60	70
		100	40	5
		200	35	5
Tachuwei (Plinthitic Paleudalf)	40	25	75	70
		50	60	70
		100	40	5
		200	35	5
Lungchung (Plinthaquic Paleudult)	40	25	75	70
		50	60	70
		100	40	5
		200	35	5
Luchu (Typic Plinthaquult)	25–30	25	68	36
		50	50	21
		100	27	21
		200	27	25
Hsinwu (Typic Plinthaquult)	30	25	40	10
		50	45	30
		100	50	30
		200	55	10
Chuwei-1 (Typic Plinthaquult)	23	25	51	63
		50	41	33
		100	45	40
		200	63	48
Houhu-1 (Typic Plinthaquult)	20	25	53	75
		50	33	55
		100	21	80
		200	38	75
Houko (Typic Paleaquult)	20	25	57	69
		50	34	53
		100	21	76
		200	38	65
Chuwei-2 (Typic Paleaquult)	18	25	55	95
		50	65	100
		100	70	100
		200	80	100
Houhu-2 (Typic Paleaquult)	15	25	55	95
		50	65	100
		100	70	100
		200	80	100

morphometrics. In the second soil group, the highest amounts of redox concentrations (≥ 30 %) were found in the Btv horizons with about 20–60 % annual saturation duration and 10–80 % annual reduction duration. These depths were probably the transitional zones between the fluctuating depths of perched irrigated water and groundwater table (Tables 10.1 and 10.2). The presence of plinthite

implied that the saturated conditions from Btv horizons are the result of long-term seasonal fluctuation of the groundwater (Daugherty and Arnold 1982). Red (2.5YR 3/6 or 4/6) and hard ferromanganiferous nodules were prevalent in these horizons. In the third soil group, the prevailing redox depletions corresponded to high annual duration of saturation (21–80 %) and reducing conditions (55–100 %) (Table 10.2). The discrepancy between ASD and ARD could be probably attributed to the clayey texture of the soils; the reduced conditions prevailed as the water table lowered. In the Luchu soil, annual duration of saturation was higher than that of reduction at a depth of 200 cm which can be attributed to the high dissolved oxygen content in groundwater under oxyaquic conditions (Hseu and Chen 2001; Jien et al. 2010).

10.3.2 Relationship Between Soil Redoximorphic Features and Hydrology

Several studies have found significant correlations between soil color and moisture regimes (Hseu and Chen 1996, 2001; Jien et al. 2004, 2010). Jien et al. (2004) found that the saturation duration of the horizon above 50 cm was not significantly correlated to soil chroma index (CI) or soil reduction duration. These results implied that the pedoturbation of the surface 50 cm resulted from human irrigation during the growing season occurred. The Fe depletions in the A horizon was difficult to identify and should be regarded as color affected by organic matter. The soil color index within 50 cm from surface soil is difficult for predicting the soil wetness condition in rice-growing soils. Significant correlations were found between the soil color index and soil saturation duration ($r = -0.43^{**}$, $p < 0.01$) and reduction duration ($r = -0.52^{**}$, $p < 0.01$) for 50–100 cm soil depth. The RMFs at this depth were affected by groundwater table and by perched water. The reduction and saturated time at this depth were >25 and >35 % of a year, and the contents of the Fe depletion ranged from 5 to 40 %. This result confirms the results of Daniel et al. (1971) and Evans and Franzmeier (1986), who found soil chroma to correlate with soil saturation at a depth of 30–60 cm.

In this study, we also divided soil layers into <30 and 30–100 cm and divided soil RMFs into GMs (value ≥ 5 , chroma ≤ 3) and red mottles (RM) (value ≥ 4 , chroma ≥ 3) to assess the correlation between soil color and soil wetness conditions including the annual saturation and reduction durations. For the surface soils (≤ 30 cm), the results revealed that neither GM nor RM existed significant correlation with annual saturation or reduction duration (Fig. 10.2). There was no obvious correlation between GM or RM and annual saturation duration in horizons below 30 cm. The significantly positive relationship existed between GM and annual reduction duration, and negative relationship was found between RM and annual reduction duration (Fig. 10.3) in horizons below 30 cm.

Soil color index provided a good morphology index for predicting soil wetness conditions at depths below 30 cm for the rice-growing soils in Taiwan, particularly

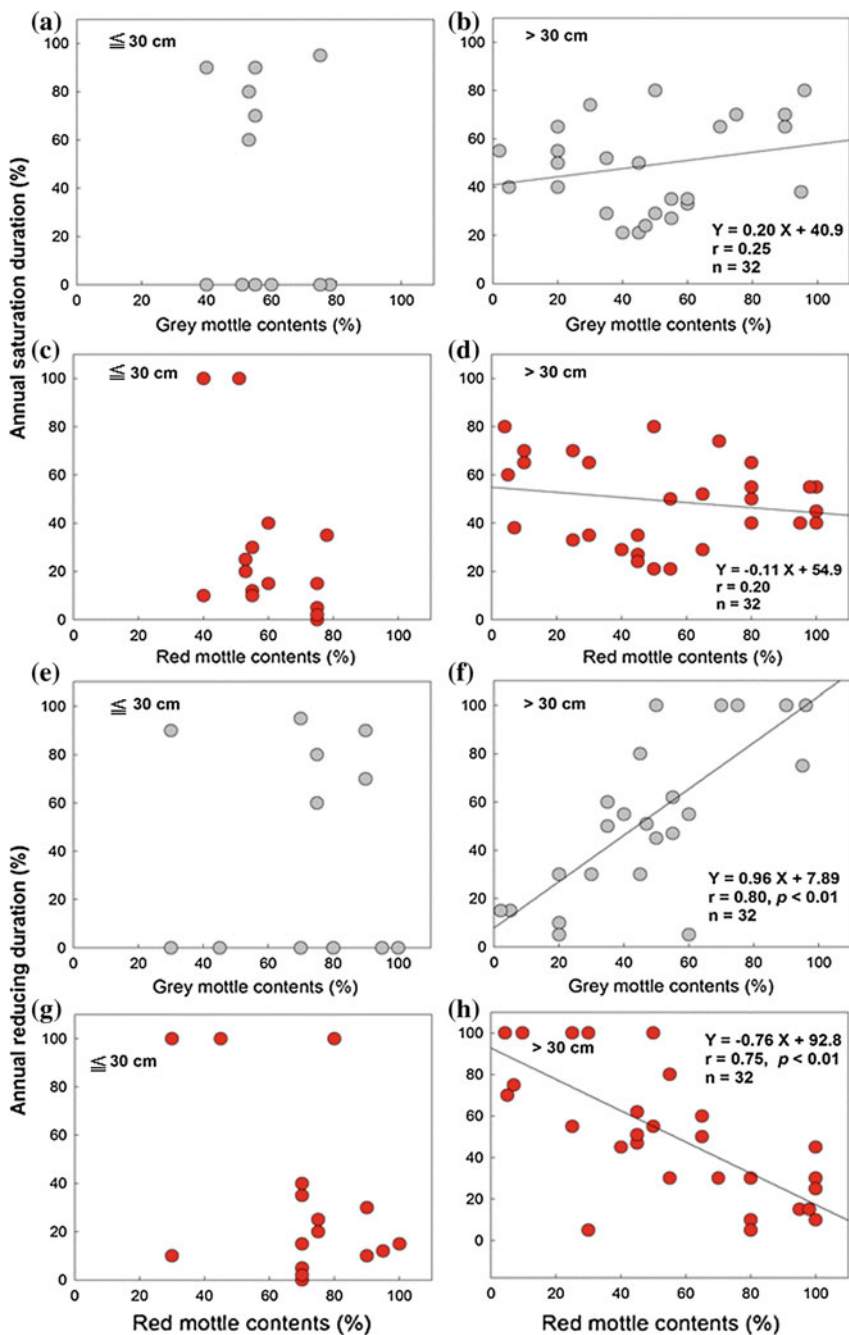


Fig. 10.3 Correlations between soil wetness conditions and redoximorphic features: **a–d** annual saturation duration (%); **e–h** annual reduction duration (%)

for annual reduction duration. The surface soil is pedoturbated resulting from rice-growing cultivation and the accumulation of rice straw residual. These phenomena create difficulties in identifying the RMFs and cause errors in correlation establishment. New digital techniques should be developed to describe and quantify RMFs to improve the correlations between soil color and soil wetness conditions.

10.3.3 *Fe, Al, and Mn and Hydrology*

Levels of iron and manganese were changing with SMR. We can use instruments, e.g., portable XRF, to estimate distribution of Fe and/or Mn in situ to predict SMR or variances of groundwater table within soil profiles.

In our studied sites, oxalate- and DCB-extractable fractions and total contents of Fe and Mn were determined in bulk soils to assess the effects of different moisture regimes for the three soil groups. Extractions of Fe and Mn were performed on some of selected pedons. The Fe extraction data suggested that the soil matrix of all analytical pedons are a source of Fe that can be reduced, translocated, and concentrated in RMFs (Table 10.3), particularly in soils of the second group. In the pedon with the highest reducing conditions (>70 % of the year), the Houko soil (the 3rd group), the contents of Fe_d were lower than those of the other two soils. The Fe_o in the Houko soil was however much higher than the other two sites, suggesting that the crystallization of free Fe was retarded by the duration of reducing conditions. This was also found by Khan and Fenton (1996). Consequently, iron activity ratio (Fe_o/Fe_d) might be suggested as an index for prediction soil moisture regimes. Table 10.4 shows a positive correlation between annual reduction duration (ARD) and Fe_o ($r = 0.31^{**}$, $p < 0.01$) and Fe_o/Fe_d ($r = 0.47^{**}$, $p < 0.01$). A significantly negative correlation ($r = -0.54^{**}$, $p < 0.01$) was also found between ARD and Fe crystalline ratio ($(Fe_d - Fe_o)/Fe_o$), indicating an estimation of soil moisture regimes by Fe contents.

The ratio of Mn_d/Fe_d in nodules is a good indicator for prediction of soil depths where the water table fluctuated, because Mn accumulated and was well crystallized at these depths. It was also found that the maximum Mn_d/Fe_d ratios of soils are found at depths of fluctuating water table. The results are corresponded with Khan and Fenton (1996), who found that the highest Mn_d/Fe_d ratio was correlated with the zones where frequent wetting and drying cycles occurred. In the Chuwei soil, the highest ratio of Mn_d/Fe_d (0.19–0.44) was in the Btv5 horizon (170–200 cm) where the groundwater table fluctuated frequently (Tables 10.1 and 10.3). In the Luchu soil, the Mn_d/Fe_d ratio ranged from 0 to 0.03 (Table 10.5). The maximum ratio was found in the Ap horizon (0–20 cm) where perched irrigated water fluctuated. The next highest ratio was found in the Btv6 horizon (160–180 cm) and the Btv3 horizon (75–104 cm) where the water table frequently fluctuated.

Table 10.3 Selected extraction of Fe and Mn of the studied pedons

Horizon	Depth	Oxalate		DCB		Total		Fe _o /Fe _d	(Fe _d -Fe _o)/Fe _t	Mn _d /Fe _d
		Fe _o	Mn _o	Fe _d	Mn _d	Fe _t	Mn _t			
<i>Lunchung</i>										
Ap	0–20	2.5	0.0	39	0.1	30	0.0	0.06	1.22	0.26
Bw	20–41	1.6	0.0	82	0.1	18	0.0	0.02	4.47	0.12
2A	41–56	2.3	0.0	42	0.1	24	0.1	0.05	1.65	0.24
2Bt	56–85	0.9	0.0	61	0.3	30	0.1	0.01	2.00	0.49
2Btv1	85–100	0.6	0.2	58	0.3	24	0.1	0.01	2.39	0.52
2Btv2	100–140	0.4	0.1	37	0.3	42	0.3	0.01	0.87	0.81
2Btv3	140–180	1.4	0.3	71	1.5	–	–	0.02	–	2.11
2Btv4	>180	1.3	0.2	72	2.0	–	–	0.02	–	2.78
<i>Luchu</i>										
Ap	0–20	2.7	0.2	20	0.3	45	0.5	0.14	0.38	1.50
Btv1	20–50	1.1	0.2	24	0.2	50	0.5	0.05	0.46	0.83
Btv2	50–75	0.9	0.2	22	0.1	48	0.4	0.04	0.44	0.45
Btv3	75–104	1.5	0.2	25	0.2	40	0.3	0.06	0.59	0.80
Btv4	104–124	1.6	0.2	29	0.1	47	0.3	0.06	0.58	0.34
Btv5	124–160	1.5	0.2	27	0.1	40	0.3	0.06	0.64	0.37
Btv6	160–180	1.9	0.2	28	0.3	44	0.4	0.07	0.59	1.07
<i>Hsinwu</i>										
Ap	0–15	2.2	0.2	36	0.1	39	0.3	0.06	0.87	0.28
AB	15–26	1.0	0.3	36	0.2	–	–	0.03	–	0.56
Bt1	26–45	0.5	0.3	45	0.2	47	0.5	0.01	0.95	0.44
Bt2	45–75	0.5	0.3	58	0.2	60	0.5	0.01	0.96	0.34
Btv1	75–107	0.8	0.2	48	0.2	50	0.4	0.02	0.94	0.42
Btv2	107–133	1.2	0.3	52	0.3	54	0.6	0.02	0.94	0.58
Btv3	133–160	1.4	0.3	52	0.3	56	0.6	0.03	0.90	0.58
<i>Chuwei-1</i>										
Ap	0–18	2.6	0.1	22	0.1	22	0.2	0.12	0.88	0.45
AB	18–36	2.5	0.1	26	0.1	26	0.2	0.10	0.90	0.38
Btv1	36–70	1.7	0.4	32	0.4	39	0.6	0.05	0.78	1.25
Btv2	70–110	1.5	0.2	37	0.2	34	0.3	0.04	1.04	0.54
Btv3	110–145	0.9	0.3	22	0.2	23	0.3	0.04	0.92	0.91
Btv4	145–170	0.5	0.0	27	0.0	29	0.1	0.02	0.91	0.00
Btv5	>170	2.6	7.2	60	6.9	66	9.2	0.04	0.87	11.5
<i>Houhu-1</i>										
Ap	0–34	2.4	0.1	29	0.1	32	0.1	0.08	0.83	0.34
AB	34–47	0.7	0.1	32	0.1	31	0.3	0.02	1.01	0.31
Bt1	47–66	0.4	0.2	45	0.2	30	0.3	0.01	1.49	0.44
Btv1	66–82	0.5	0.4	53	0.3	44	0.1	0.01	1.19	0.57
Btv2	82–102	0.6	0.3	56	0.5	56	0.7	0.01	0.99	0.89
Btv3	102–122	1.0	0.3	61	0.3	63	0.7	0.02	0.95	0.49
Btv4	122–150	0.8	0.3	52	0.3	56	0.5	0.02	0.91	0.58
<i>Houko</i>										
Ap	0–20	5.2	0.1	26	0.2	35	0.3	0.20	0.59	0.77
Bt1	20–50	2.4	0.3	23	0.1	74	0.5	0.10	0.28	0.43
Bt2	50–75	3.6	0.2	21	0.2	49	0.4	0.17	0.36	0.95
Bt3	75–110	8.3	0.2	24	0.2	76	0.4	0.35	0.21	0.83
Btg1	110–130	17	0.3	18	0.2	39	0.5	0.94	0.03	1.11
Btg2	130–170	3.1	0.1	36	0.2	74	0.3	0.09	0.44	0.56

–: Not available

Fe_d: DCB extraction (g/kg)Fe_o: Oxalate extraction (g/kg)Fe_t: Total amount of elements (g/kg)

Table 10.4 Pearson correlation coefficient among soil properties, soil wetness conditions, and redoximorphic feature amounts

	Clay	Fe _d	Mn _d	Fe _o	Mn _o	Fe _t	Mn _t	Fe _o /Fe _d	(Fe _d -Fe _o)/Fe _t	ASD	ARD	GM	RM
Clay	1.00												
Fe _d	0.24	1.00											
Mn _d	0.34*	0.28*	1.00										
Fe _o	-0.04	-0.35**	-0.01	1.00									
Mn _o	0.30*	0.21	0.98**	0.01	1.00								
Fe _t	0.01	0.66**	0.21	-0.05	0.19	1.00							
Mn _t	0.29*	0.29*	0.99**	0.00	0.98**	0.29*	1.00						
Fe _o /Fe _d	-0.07	-0.43**	-0.07	0.98**	-0.05	-0.15	-0.06	1.00					
(Fe _d -Fe _o)/Fe _t	0.24	0.48**	0.13	-0.62**	0.07	-0.24	0.07	-0.62**	1.00				
ASD	-0.23	0.16	0.06	-0.12	0.06	0.17	0.08	-0.14	0.10	1.00			
ARD	-0.08	-0.34*	-0.02	0.41**	0.04	0.06	0.01	0.37**	-0.54**	0.26*	1.00		
GM	0.27	0.02	0.02	0.16	0.01	0.41*	0.03	0.12	-0.32*	-0.23	0.25	1.00	
RM	0.32*	0.06	0.32*	0.14	0.30	0.07	0.32*	0.13	-0.01	-0.12	-0.16	-0.01	1.00

–; Not available; Fe_d: DCB extraction; Fe_o: oxalate extraction; Fe_t: total amount of elements; ASD: annual saturation duration; ARD: annual reduction duration; GM: gray mottle amounts; RM: red mottles

* $p < 0.05$

** $p < 0.01$

Table 10.5 Types and quantities of redoximorphic features identified by naked eye and image analysis

Chuwei pedon	Matrix color	Fe depletions		Fe concretions		
		Gray (%)	Light yellow (%)	Yellow (%)	Yellow (%)	Red (%)
<i>Naked eye</i>						
Ap	10YR 4/3 (95)	2.5Y 3/1 (1)	–	10YR 6/8 (2)	–	5YR 5/8 (2)
AB	10YR 4/1 (91)	2.5Y 3/1 (2)	–	7.5YR 5/8 (2)	–	5YR 5/8 (5)
Btv1	N 6/0 (35)	–	–	10YR 5/8 (20)	–	5YR 5/8 (45)
Btv2	N 6/0 (55)	–	10YR 7/8 (20)	7.5YR 6/8 (25);	–	–
<i>Image analysis</i>						
Ap	10YR 4/3 (43)	10YR 6/1 (5)	7.5YR 6/3 (19)	5YR 6/8 (16)	–	10R 4/8 (17)
AB	10YR 4/1 (45)	10YR 6/1 (10)	–	7.5YR 7/8 (23)	2.5YR 4/8 (10)	10R 4/8 (12)
Btv1	10YR 7/1 (54)	–	10YR 7/3 (13)	7.5YR 7/6 (15)	–	2.5YR 5/8 (18)
Btv2	10YR 6/1 (42)	–	10YR 7/3 (24)	7.5YR 6/8 (34)	–	–

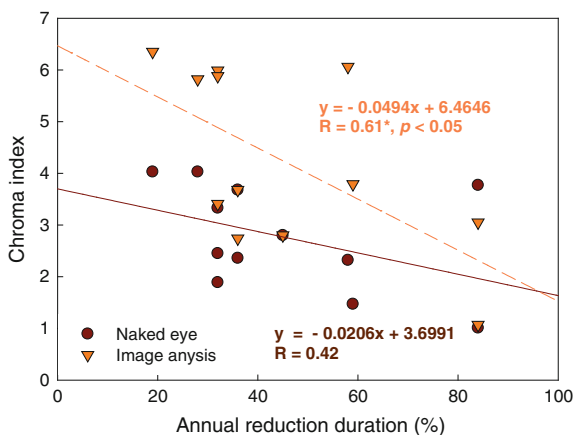
– : None

10.3.4 Digitize Redoximorphic Features

There was significant correlation between ARD and CI (Jien et al. 2004), as well as ARD and GM/RM contents (Fig. 10.3). Jien et al. (2004) indicated that the presence of organic carbon would lead to misjudgment and content misestimate of RMFs in upper soil horizons (<50 cm depth) if we identified and quantified the features by naked eyes in situ. A digital technique could be developed to precisely describe and quantify soil morphologies like applying image analysis techniques or spectroscopic estimates though Vis–NIR (Viscarra Rossel et al. 2009).

This study collected soil blocks (10 × 10 × 10 cm) from each horizon and then cut each block into 10 soil pieces (1 cm thick) for image analysis by IMAGIN 8.4. From the image analysis, the detail information of types and amounts of RMF was acquired. For Chuwei-1 soil, Table 10.5 compares with the identified types and amounts of RMFs by methods of naked eye and image analysis. Large differences of RMFs identification were found in Ap and AB horizons. The gray (10YR 6/1), reddish yellow (5YR 6/8 or 7.5YR 7/8), and red (10YR 4/8) seem to be misjudged by naked eye (Table 10.5), and the largest amounts of the misjudged RMFs ranged

Fig. 10.4 Regression correlations between chroma index (*CI*) and annual reduction duration: *orange line* is image analysis method, and *brown line* is naked eye method



from 46 to 52 % in this study. Such misjudgments might be the major reason why soil colors fail to correlate to moisture regimes in surface soils (<30 cm). Our hypothesis is demonstrated in Fig. 10.4, in which significant negative correlation between ARD and CI was calculated from identified RMFs by image analysis. The CI values from RMFs identified by naked eye method failed to correlate to ARD in surface soils.

10.4 Conclusions

Digital soil morphometrics can help measuring and quantifying soil profile attributes and deriving continuous depth functions for further soil understanding. This study established correlations between soil color and wetness condition in rice-growing soils in Taiwan to help us in clarifying the SMR and develop criteria for classifying these soils. The study indicated that soil color could be used to assess soil wetness within soil profile as well as selective extraction of Fe and Mn. Digital soil morphometrics using image analysis significantly increased precision in quantifying and qualifying soil morphology.

Acknowledgements The authors would like to thank the Ministry of Science and Technology of the Republic of China (Taiwan) for financially supporting this research under Contract No. MOST 103-2313-B-020-007-MY2.

References

- Ben-Dor E, Heller D, Chudnovsky A (2008) A novel method of classifying soil profiles in the field using optical means. *Soil Sci Soc Am J* 72:1113–1123
- Blake GR, Hartge KH (1986) Bulk density. In: Klute A (ed) *Methods of soil analysis*. Part 1, 2nd edn., ASA and SSSA, Madison, WI, pp 363–375 (Agron. Monogr. 9)
- Cox JW, Fritsch E, Fitzpatrick RW (1996) Interpretation of soil features produced by ancient and modern process in degraded landscapes VII. Water duration. *Aust J Soil Res* 34:803–824
- Dematté JAM, Campos RC, Alves MC, Fiorio PR, Nanni MR (2004) Visible–NIR reflectance: a new approach on soil evaluation. *Geoderma* 121:95–112
- Daniel RB, Gamble EE, Nelson LA (1971) Relations between soil morphology and water-table levels on a dissected North Carolina Coastal Plain surface. *Soil Sci Soc Am Proc* 35:781–784
- Daugherty LA, Arnold RW (1982) Mineralogy and iron characterization of plinthitic soils on alluvial landforms in Venezuela. *Soil Sci Soc Am J* 46:1244–1252
- Evans CV, Franzmeier DP (1988) Color index values to represent wetness and aeration in some Indiana soils. *Geoderma* 41:353–363
- Fanning DS, Fanning MCB (1989) Gleization. *Soil morphology, genesis, and classification*. Wiley, New York, pp 110–125
- Faulkner SP, Patrick WH Jr (1992) Redox processes and diagnostic wetland indicators in bottomland hardwood forests. *Soil Sci Soc Am J* 56:856–865
- Franzmeier DP, Yahner JE, Steinhardt GC, Sinclair HR (1983) Color patterns and water table levels in some Indiana soils. *Soil Sci Soc Am J* 47:1196–1202
- Hartemink A, Minasny B (2014) Towards digital soil morphometrics. *Geoderma* 230–231:305–317
- Ho CS (1988) An introduction to the geology of Taiwan and explanation text of the geological map of Taiwan, 2nd ed. The Ministry of Economics Affairs, Republic of China, Taipei, Taiwan
- Hossner LR (1996) Dissolution for total elemental analysis. In: Sparks DL et al (eds) *Methods of soil analysis*, Part 3. Chemical methods. ASA and SSSA, Madison, WI, USA, pp 49–64
- Hseu ZY, Chen ZS (1996) Saturation, reduction, and redox morphology of seasonally flooded Alfisols in Taiwan. *Soil Sci Soc Am J* 60:941–949
- Hseu ZY, Chen ZS (2001) Quantifying soil hydromorphology of a rice-growing Ultisol topequence in Taiwan. *Soil Sci Soc Am J* 65:270–278
- Jien SH, Hseu ZY, Chen ZS (2004) Relations between morphological color index and soil wetness condition of anthraquic soils in Taiwan. *Soil Sci* 169:871–882
- Jien SH, Hseu ZY, Chen ZS (2010) Hydropedological implications of ferromanganiferous nodules in rice-growing plinthitic Ultisols under different moisture regimes. *Soil Sci Soc Am J* 74:880–891
- Khan FA, Fenton TE (1996) Secondary iron and manganese distributions and aquatic conditions in a Mollisol catena of central Iowa. *Soil Sci Soc Am J* 60:546–551
- Mehra OP, Jackson ML (1960) Iron oxides removed from soils and clays by a dithionite-citrate system buffered with sodium bicarbonate. *Clays Clay Miner* 7:317–327
- McKeague JA, Day JH (1966) Dithionite- and oxalate-extractable Fe and Al as aids in differentiating various classes of soils. *Can J Soil Sci* 45:49–62
- Ponnamperuma FN (1972) The chemistry of submerged soils. *Adv Agron* 24:29–96
- Schwertmann U, Fanning DS (1976) Iron and manganese concretions in hydrosequences of soils in loess in Bavaria. *Soil Sci Soc Am J* 40:731–738
- Simonson GH, Boersma L (1972) Soil morphology and water table relations. II. Correlation between annual water fluctuations and profile features. *Soil Sci Soc Am Proc* 36:649–653
- Soil Survey Staff (1993) Examination and description of soils in the field. In: *Soil survey manual*, Issued Oct 1993. Handbook No. 18. USDA-SCS, Washington, D.C, pp 59–196
- Soil Survey Staff (2010) Keys to soil taxonomy. USDA-NRCS, 11th edn. U.S. Gov. Print. Office, Washington, D.C.
- Stockmann U, Minasny B, McBratney AB (2014) How fast does soil grow? *Geoderma* 216:48–61

- Vepraskas MJ (1992) Redoximorphic features for identifying aquic conditions. Tech. Bull. 301. North Carolina Agric. Res. Serv., North Carolina State Univ., Raleigh
- Viscarra Rossel RA, Cattle SR, Ortega A, Fouad Y (2009) In situ measurements of soil colour, mineral composition and clay content by vis-NIR spectroscopy. *Geoderma* 150:253–266
- Viscarra Rossel RA, Webster R (2011) Discrimination of Australian soil horizons and classes from their visible-near infrared spectra. *Eur J Soil Sci* 62:637–647